Theory and simulation of central force model potentials: Application to homonuclear diatomic molecules

Cite as: J. Chem. Phys. **105**, 10008 (1996); https://doi.org/10.1063/1.472833
Submitted: 05 August 1996 . Accepted: 05 September 1996 . Published Online: 04 June 1998

Fernando Bresme, José L. F. Abascal, and Enrique Lomba

Theory and simulation of central force model potentials: Application to homonuclear diatomic molecules

Fernando Bresme
Departamento de Química-Física, Facultad de Ciencias Químicas, Universidad Complutense de Madrid, E-28040, Spain and Instituto de Química-Física Rocasolano, CSIC, Serrano 119, E-28006 Madrid, Spain

José L. F. Abascal
Departamento de Química-Física, Facultad de Ciencias Químicas, Universidad Complutense de Madrid, E-28040, Spain

Enrique Lomba
Instituto de Química-Física Rocasolano, CSIC, Serrano 119, E-28006 Madrid, Spain

(Received 5 August 1996; accepted 5 September 1996)

Structure and thermodynamics of fluids made of particles that interact via a central force model potential are studied by means of Monte Carlo simulations and integral equation theories. The Hamiltonian has two terms, an intramolecular component represented by a harmonic oscillatorlike potential and an intermolecular interaction of the Lennard-Jones type. The potential does not fulfill the steric saturation condition so it leads to a polydisperse system. First, we investigate the association (clustering) and thermodynamic properties as a function of the potential parameters, such as the intramolecular potential depth, force constant, and bond length. It is shown that the atomic hypernetted chain (HNC) integral equation provides a correct description of the model as compared with simulation results. The calculation of the HNC pseudospinodal curve indicates that the stability boundaries between the vapor and liquid phases are strongly dependent on the bond length and suggests that there might be a direct gas–solid transition for certain elongations. On the other hand, we have assessed the ability of the model to describe the thermodynamics and structure of diatomic liquids such as N_2 and halogens. To this end we have devised a procedure to model the intramolecular potential depth to reproduce the complete association limit (i.e., an average number of bonds per particle equal to one). This constraint is imposed on the Ornstein–Zernike integral equation in a straightforward numerical way. The structure of the resulting fluid is compared with results from molecular theories. An excellent agreement between the HNC results for the associating fluid and the reference interaction site model (RISM)-HNC computations for the atom–atom model of the same fluid is obtained. There is also a remarkable coincidence between the simulation results for the molecular and the associating liquids, despite the polydisperse character of the latter. The stability boundaries in the complete association limit as predicted by the HNC integral equation have been computed for different bond lengths corresponding to real molecular liquids. These boundaries appear close to the experimental liquid branch of the vapor–liquid coexistence line of the molecular systems under consideration. [S0021-9606(96)50646-X]

I. INTRODUCTION

Central force potentials (CFM) are useful models to describe molecular systems. These Hamiltonians are interesting because molecules are not defined explicitly. One deals with a mixture of atoms or ions that eventually can react to give a mixture of atoms/ions and molecules which in turn may dissociate. Maybe one of the most illustrative examples of this type of Hamiltonian is the central force model of water devised 20 years ago by Stillinger and co-workers.[1] This potential was used in the context of molecular dynamics (MD) simulations and it has shown to be a good model in the description of the water properties at ordinary conditions of temperature and density. The simplicity of the potential and the fact that chemical association was implicit in the model induced some authors[2–4] to approach the CFM from a theoretical standpoint in the context of the atomic Ornstein–Zernike (OZ) integral equation. One immediate advantage of this potential model would be to avoid the cumbersome treatment of angular correlations which appear when molecules are considered explicitly. Thuraisingham and Friedman[3] solved for the first time the CFM of water at room temperature. There, the limitations of the HNC integral equation to cope with the complex structure of the liquid were exposed. The main difficulties were related to the inability of the integral equation to describe correctly the number of intramolecular bonds in the molecule, as well as its poor description of the hydrogen bond correlations. More recent studies[4,5] have tried to solve the same Hamiltonian with improved theories but a correct theoretical description is still missing. Besides, it is not yet clear whether the difficulties are inher-

 0021-9606/96/105(22)/10008/14/$10.00

ent to the peculiarities of the water molecule, i.e., whether similar problems would arise or not when dealing with molecules without hydrogen bonds.

Central force models, included that of water, are by construction effective potentials which give rise to association. Following the pioneering works by Wertheim,[6,7] a number of simple models for the investigation of associating liquids have been proposed and discussed recently.[8–13] The extension of these studies to charged systems was done using the sticky electrolyte model.[14–16] The association degree is determined by the Boltzmann weighting factor, and at a first glance there is no reason to believe that this potential would lead to complete association, i.e., to a system exclusively composed by molecules. The problem to be solved will then be that of a chemical reaction between two species, for instance in water H^+ and O^{2-} species to give H_2O. In the terminology of Cummings and Stell[10] the statistical mechanics models of chemical reactions consider the inhomogeneous association reaction $A+B \rightleftharpoons AB$ as well as its homogeneous counterpart $2A \rightleftharpoons A_2$.[11] The Hamiltonians employed, both in neutral and charged systems, aside from being of the central force model type, shared a common feature, as is the possibility of analytically solving the problem within the OZ integral equation context subject to a certain closure. Using this analytical approach, the authors investigated the equilibrium constant of the association reaction as a function of the density and temperature. These studies included the case of infinite equilibrium constant, i.e., the case when diatomic molecules are the only species present in the system. This fact is possible in a heterogeneous association reaction if the Hamiltonian enables the steric saturation feature.[10] This particular case represents an alternative to study molecular systems from a theoretical point of view.

It is apparent that the theoretical solution of the CFM potentials using the atomic OZ integral equation is a problem of the same type as considered previously by other authors. Unfortunately, the complex nature of realistic CFM potentials precludes the analytical solution of the problem as early noted by Cummings and Stell.[10] Therefore, one is forced to adopt a numerical procedure that guarantees the complete association limit. In this work we have studied the problem of a *homogeneous* association reaction, $A \rightleftharpoons A_2 \rightleftharpoons \cdots \rightleftharpoons A_n$. The system in equilibrium is then a polydisperse mixture of species. We are also interested in a particular limit of this reaction corresponding to the case $2A \rightarrow A_2$. Our system is made of neutral particles that interact through a potential, including a Lennard-Jones term, which describes the intermolecular interactions, and a harmonic oscillator contribution, which allows for the chemical association of the particles. Depending on the depth of the intramolecular potential the chemical equilibrium is shifted toward different association constants. In this way the potential leads to polydisperse systems. We will investigate by computer simulation the properties of this type of association reaction. Despite the intrinsic polydisperse nature of these systems, we will show that the model is useful in the study of several homonuclear diatomic molecules—nitrogen, halogens—when the question is addressed in terms of a state equivalent to the complete association limit. We do this by requiring that the mean number of bonds per particle be one. The condition translates into the calculation of the value of the intramolecular potential depth leading to the ''complete association limit.'' Once such a parameter of the intramolecular potential is obtained, we make a double comparison. First, we solve the atomic HNC integral equation of that system and compare it with the corresponding Monte Carlo results and with the predictions from molecular theories, such as the reference interaction site model (RISM).[17–19] On the other hand, we check whether the central force model with the complete association constraint is able to predict the behavior of real diatomic liquids.

In a first part of this work we describe the Hamiltonian and the relevant methodology of the simulations performed and the integral equation calculations. We also give the definition of the essential quantities used along the work as well as concepts such as the *complete association* limit. Next we study the stability boundaries of the HNC integral equation for the Hamiltonian as a function of the bond length. Then the association reaction for the *homogeneous* case is considered both from theory and Monte Carlo simulations. We devote the following section to the study of the complete association limit attained by imposing a constraint on the *mean* number of bonds per particle to the integral equation theory. Finally, we present structural results obtained from the atomic OZ integral equation in the complete association limit for realistic diatomic molecules, and compare these results with previous computations using molecular theories. This section is complemented with the theoretical calculation of the stability boundaries obtained for the complete association case and its comparison with the experimental liquid branch of homonuclear diatomic molecules. Main conclusions and lines of future development close this paper.

II. CENTRAL FORCE MODEL AND CHEMICAL ASSOCIATION

We consider a system made of particles interacting through a central force model type Hamiltonian. This potential consists of two terms, one representing the intramolecular interactions and another one accounting for the intermolecular forces. The intermolecular part, usually in the study of rigid diatomic molecules, is modeled by means of a simple Lennard-Jones potential:

$$u_{\text{inter}}(r) = 4\epsilon\left[\left(\frac{\sigma}{r}\right)^{12} - \left(\frac{\sigma}{r}\right)^{6}\right], \tag{1}$$

where σ and ϵ are the well-known parameters defining the particle diameter and the potential depth, respectively. These parameters are used to define the reduced temperature $T^* = k_B T/\epsilon$, k_B being the Boltzmann constant, and the reduced density, $\rho^* = N\sigma^3/V$, where N represents the total number of particles filling a volume V. The intramolecular part enabling the association of the particles is modeled through a simple harmonic oscillatorlike function,

$$u_{\text{intra}}(r) = \tfrac{1}{2}\, k(r-L)^2 + D_e, \tag{2}$$

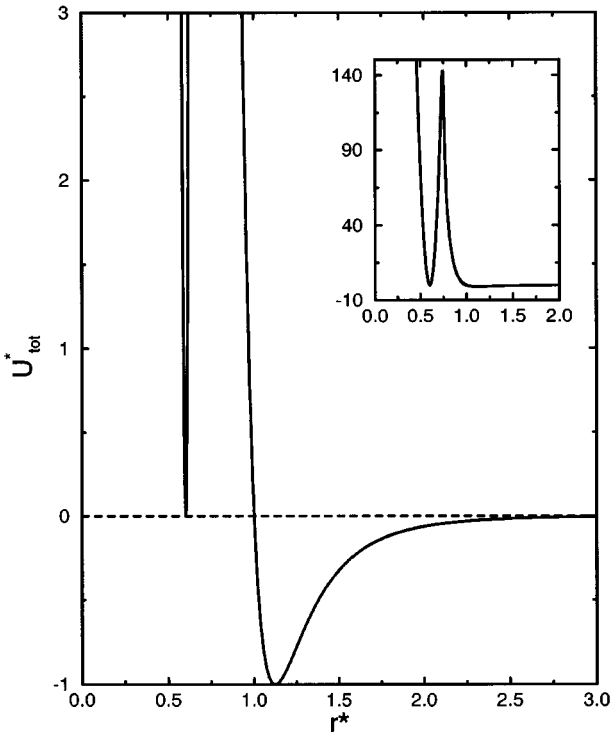

FIG. 1. Central force model potential for $L^*=0.6$, $D_e^*=0$, and $k^*=15\,000$ [see Eq. (4)]. As throughout this work, $R^*=0.75$ and $w^*=0.015$.

where k is the force constant of the bond, L is the bond length, and D_e is the intramolecular potential depth. Using the values of σ and ϵ defined above we can write $u^*=u/\epsilon$, $k^*=k\sigma^2/\epsilon$, $L^*=L/\sigma$, $D_e^*=D_e/\epsilon$, and $r^*=r/\sigma$. In addition, we define a switching function which has the effect of interpolating between the intramolecular and the intermolecular potential

$$l(r)=\frac{1}{2}\left[1+\tanh\left(\frac{r-R}{w}\right)\right]. \tag{3}$$

The parameters R and w tune the location and the steepness of the switching function. A small value for w leads to an abrupt change from the intramolecular to the intermolecular interaction. Throughout this work we have used the values $R=0.75\sigma$ and $w=0.015\sigma$. Taking into account all the above functions, the total potential energy has the form

$$u_{\mathrm{tot}}(r)=[1-l(r)]u_{\mathrm{intra}}(r)+l(r)u_{\mathrm{inter}}(r). \tag{4}$$

In Fig. 1 we depict this function for the case $L^*=0.6$ and $k^*=15\,000$. As a comparison, in Table I we compile the values of the bond length, L^*, and the force constant, k^*, as well as the ϵ and σ parameters suitable to model several homonuclear diatomic molecules.[20,21] The choice for D_e determines the extent of the association reaction. Different values will be used depending on whether the complete association limit is to be fulfilled or not. For the case of an association reaction in which diatomic molecules are not the only species present, the simple value $D_e=0$ has been chosen. It must be pointed out that in the limit $k\to\infty$ the intramolecular potential has zero width, the same as that used by Cummings and Stell.[10,11] For $k^*=15\,000$ the thermal barrier between the intramolecular and the intermolecular potentials is about 150ϵ (cf. Fig. 1). Given the magnitude of the wall we can expect a small difference between the results obtained in this way and those considering an infinite thermal barrier.

TABLE I. Potential parameters.

Molecule	(ϵ/k_B)/K	σ/Å	L^*	k^*
N_2[a]	37.3	3.310	0.329	487903
F_2[b]	52.8	2.825	0.505	51744
Cl_2[b]	173.5	3.353	0.608	15140
Br_2[b]	257.2	3.538	0.630	8673

[a]σ and ϵ values taken from Ref. 20.
[b]σ and ϵ values taken from Ref. 21.

Let us consider the homogeneous association reaction,

$$A\rightleftharpoons A_2\rightleftharpoons\cdots\rightleftharpoons A_n\,. \tag{5}$$

Now some criterion must be introduced in order to consider two particles associated. Here, we have adopted a structural definition according to which two particles are deemed associated if the distance between their centers is less than a given separation R_b. The running coordination number, $\langle N\rangle$, is the average number of atoms up to R_b,

$$\langle N\rangle=4\pi\rho\int_0^{R_b}g(r)r^2\,dr, \tag{6}$$

where $g(r)$ is the pair correlation function. As discussed by Cummings and Stell[10] for a simpler but similar potential, the homogeneous reaction stops in the formation of dimers only if the pair potential exhibits the property of *steric saturation*, i.e., the potential is such that each atom can belong to *at most* one diatomic molecule. When the system is a mixture of two species A and B, the steric saturation can be fulfilled just by considering that there are no intramolecular interactions between like particles. In addition to this, the bond length must fulfill $L<\sigma/2$. This is not the case of the homogeneous association reaction. Even for elongations $L^*<1/2$ trimers and tetramers (with the particles placed at the vertices of regular triangles and tetrahedra) can be formed. For $L^*\geqslant 1/2$ there is an increasing probability of formation of clusters of size larger than two. Thus, the value $\langle N\rangle=1$ is an unambiguous indication of the complete association into diatomic molecules only under some circumstances. Nevertheless, as $\langle N\rangle$ represents the average number of bonds per particle, such value represents a state somewhat similar to that defined by the complete association for systems fulfilling the steric condition. Hereafter we will refer to the condition $\langle N\rangle=1$ as the *complete association limit*. Since the particles can polymerize in clusters of various sizes, it is interesting to know the cluster population of the system in the full association limit. At the same time it should be possible to assess the ability of a theory that relies on such a condition to describe a real diatomic system. Notice that the cluster population is not a property easily accessible from theory. On the contrary, the evaluation of cluster populations is trivial in computer simu-

lations. If the agreement between thermodynamic and structural results of theory and simulation were good enough, the cluster population obtained from simulation could be taken as representative of the system described by the theory.

III. MONTE CARLO AND MOLECULAR DYNAMICS SIMULATIONS

Monte Carlo simulations have been performed in the canonical ensemble. Implementation of these simulations is a trivial exercise (see for instance Ref. 22). Only some care must be taken in the high density regime in order to correctly sample the phase space. Due to the double nature of the potential, i.e., intramolecular and intermolecular, one is compelled to use a particle displacement large enough to allow that a particle escapes from the intramolecular well. So we have chosen to set the maximum displacement to $\delta r=0.7\sigma$. Of course, a displacement like that has the effect of drastically diminishing the number of accepted configurations and, consequently, produces a poor sampling of the phase space in high density systems. The sampling of the intermolecular interactions is needed as well. We have introduced an additional maximum displacement distance, $\delta r=0.15\sigma$, a value usually adopted in the simulation of high density fluid systems. In summary, for each new Monte Carlo (MC) step we randomly choose the maximum displacement distance to be either 0.15σ or 0.7σ. It must be stressed that the use of two maximum displacements for the movement of the particles still fulfills the detailed balance equation. The procedure typically turns out in an acceptance rate close to 10%. Simulations at low densities use half the box length as maximum displacement, which results in acceptance rates around 50%. Properties are typically accumulated in 50 subaverages of approximately 10^5 particle movements each. These are used to compute the standard deviation of the properties such as internal energy, pressure, or intramolecular coordination number, $\langle N\rangle$ (obtained by integration of the intramolecular peak of the pair correlation function). The equilibration period lasted between $10^4\times N_{\text{particles}}$ and $2\times10^4\times N_{\text{particles}}$ movements, being $N_{\text{particles}}=216$ in all the cases studied. The cutoff distance is set to 2.8σ.

By means of molecular dynamics (MD) in the microcanonical ensemble[23] we have simulated a set of particles which interact via the potential described in Sec. II. This is a conventional simulation in the sense that no constraints are included in order to preserve the molecular entity. Usually, the initial configuration consisted in 108 molecules arranged in an fcc lattice. During the simulation we did not observe any dissociation as this event is extremely improbable given the thermal barrier existing between the intermolecular and intramolecular potential contributions. Notice that the use of MD in the case of CFM potentials then has the peculiarity of giving the properties of a system which is not in its minimum of free energy, contrary to what happens in our Monte Carlo simulations. The integration of the equations of motion was done using the velocities Verlet's algorithm, with a time step $\delta t^*=0.005$ in Lennard-Jones parameters units. The cutoff was set to half the box length.

IV. INTEGRAL EQUATIONS

The theoretical treatment used in this work deals with the solution of the well-known atomic Ornstein–Zernike (OZ) equation, which in its general form for multicomponent systems reads

$$h_{\alpha\nu}(\mathbf{r})=c_{\alpha\nu}(\mathbf{r})+\sum_l \int c_{\alpha l}(\mathbf{r}')h_{l\nu}(|\mathbf{r}-\mathbf{r}'|)d\mathbf{r}', \tag{7}$$

being $h_{\alpha\nu}=g_{\alpha\nu}-1$ the total correlation function, $g_{\alpha\nu}$ the pair correlation function, and $c_{\alpha\nu}$ the direct correlation function. As usual we define the indirect correlation function $\gamma_{\alpha\nu}=h_{\alpha\nu}-c_{\alpha\nu}$. The OZ integral equation can only be solved if it's supplemented with the so-called closure relation

$$g_{\alpha\nu}=\exp(\gamma_{\alpha\nu}-\beta u_{\alpha\nu}+B_{\alpha\nu}), \tag{8}$$

where $\beta=1/k_BT$ and $B_{\alpha\nu}$ is the bridge function. Approximations to $B_{\alpha\nu}$ give rise to different integral equation theories, the simplest being the hypernetted chain (HNC) integral equation, $B_{\alpha\nu}=0$. In this work we solve the OZ equation coupled with this closure relation.

The Ornstein–Zernike equation can be written in a more compact notation in the Fourier space, namely

$$\tilde{\mathbf{H}}(k)=\tilde{\mathbf{C}}(k)[\mathbf{I}-\tilde{\mathbf{C}}(k)]^{-1}, \tag{9}$$

where $\mathbf{I}$ is the identity matrix. $\tilde{\mathbf{H}}$ is a matrix with elements $\tilde{H}_{\alpha\nu}(k)=(\rho_\alpha\rho_\nu)^{1/2}\tilde{h}_{\alpha\nu}(k)$, and analogously for the direct correlation function. Besides, the tilde denotes a three-dimensional Fourier transform. The resulting set of nonlinear equations has been solved by the method proposed by Labik, Malijevsky, and Vonka.[24] The solution renders the pair correlation function and the thermodynamic properties of the system for a given temperature and density. From the latter, and using Eq. (6), we can monitor the association reaction. As discussed in Sec. II, the use of that expression as an estimation of the number of dimers is rigorous only in the case of steric saturation in the pair potential. Otherwise it will be an approximation which will become poorer as the proportion of clusters of size larger than two is favored, i.e., as the bond length increases. The condition of complete association, $\langle N\rangle=1$ is attained by the system at different values of pairs density temperature depending, for a given intermolecular interaction, on the width, position (bond length), and depth of the intramolecular potential. If one alters the depth of the intramolecular potential, D_e, it is possible to attain complete association, $\langle N\rangle=1$, for any value of temperature and density, as long as the theory is solvable in those conditions. Actually, a change in D_e has the effect of modifying the mass action association reaction constant. For a given density and temperature, the problem to be solved is, therefore, to find the effective potential, i.e., the value for D_e, that produces $\langle N\rangle=1$. Unlike the case of Cummings and Stell's model,[10,11] which is analytically tractable, we must resort to a numerical algorithm.

This has been solved using a Newton–Raphson (NR) method, which for a thermodynamic state warrants the condition $\langle N\rangle=1$. In short, the steps are the following. First, solve the HNC equation for a given thermodynamic state.

The calculated $g(r)$ is used to obtain $\langle N\rangle$ via Eq. (6). The next step consists in searching for the D_e value in Eq. (2) such that $\langle N\rangle=1$. This is done by a standard NR formula, $D_{e,i+1} = D_{e,i} - \langle N\rangle_i/\langle N\rangle_i'$, where the $D_{e,i+1}$ is the new approximation to the desired value. The local derivative $\langle N\rangle_i'$ can be obtained numerically from the the coordination numbers for two values of D_e close enough. The procedure is finished when $\delta=|D_{e,i+1}-D_{e,i}|$ is smaller than a given value δ. We have chosen $\delta=10^{-5}$ in this application.

V. THE ASSOCIATION REACTION IN THE CASE $D_E=0$

A. Stability boundaries

Prior to obtain the results for the association reaction we have analyzed the possible influence of k^* on the thermodynamic and association properties of the system. For that purpose we have solved the HNC approximation for $L^*=1/3$, $D_e^* = 0$, and two different k^* values, namely, 15 000 and 500 000. Note that the latter value roughly corresponds to N_2 (see Table I). As can be observed in Fig. 2(a), the excess internal energy is almost insensitive to the force constant contrary to the results for pressure which exhibits remarkable differences at high densities. Larger discrepancies are observed [cf. Fig. 2(b)] for the reduced inverse isothermal compressibility $\chi_T^{-1}=(\rho k_B T\kappa_T)^{-1}$, κ_T being the isothermal compressibility. This exhibits an interesting behavior. First, it presents a minimum around $\rho^*=0.3$ which is due to the neighborhood of the critical point. An increase in density is followed by an increase in χ_T^{-1} but this is rapidly compensated, resulting in the appearance of a maximum. This is more apparent in the $k^*=15\,000$ case. Such behavior indicates the proximity of an instability region characterized at high densities by a pseudospinodal. The case $k^*=500\,000$ exhibits qualitatively similar trends but the location of the instability is shifted toward higher densities. The effect of a larger force constant, or in other words, a narrower intramolecular potential, is clearly shown in Fig. 2(c), where the value of $\langle N\rangle$ is represented for the two cases mentioned above. Association at low densities is more favored in the $k^*=15\,000$ case. At higher densities both curves rise parallel with a roughly linear dependence on density. This indicates that association at high densities is mostly a consequence of the increased encounter probability. Since we are mainly interested in the high density regime, and given that association is not qualitatively affected by the width of the intramolecular potential well, we set $k^*=15\,000$ as the common value for the remaining calculations. This choice has the positive side effect of reducing the large number of grid points needed in the resolution of the Ornstein–Zernike integral equation that would otherwise arise as a result of the smaller grid needed to cope numerically with a narrow intramolecular potential well. Consequently, in the potential of Eq. (4) the only reduced variable which discriminates among different systems is the elongation.

In view of the behavior exhibited by the inverse isothermal compressibility, we have mapped out the pseudospinodal curve obtained from the HNC integral equation as a function of the bond length. We recall that, as pointed out by

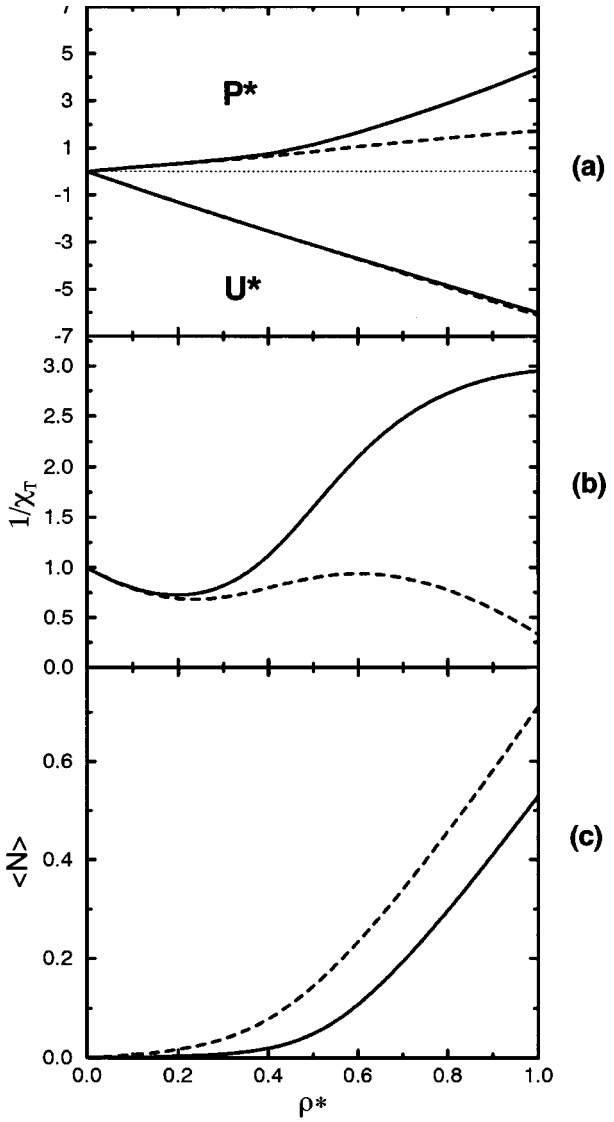

FIG. 2. Excess internal energy, pressure, reduced inverse isothermal compressibility, and mean running coordination number as a function of density at $T^*=2$. The intramolecular parameters are $D_e^* = 0$, $k^*=500\,000$ (solid lines) and $k^*=15\,000$ (dashed lines).

Belloni,[25] the HNC does not exhibit a true spinodal line, although the appearance of this pseudospinodal can be taken as a signature of instability, in most cases related to a coexistence boundary. This is particularly significant at the high density side of the pseudospinodal where the deviations from a true spinodal line are minimal. We have adopted as a pseudospinodal curve the locus of pairs of ρ^* and T^* for which $\mathbf{I}-\tilde{\mathbf{C}}(0)\propto\chi_T^{-1}=(\rho k_B T\kappa_T)^{-1}\rightarrow 0$. The key question is then which is the influence of the association on the stability boundaries of the system. In Fig. 3 we present the pseudospinodal lines as predicted by the HNC integral equation for $L^*=1/3$ and $L^*=1/2$. As a reference we also include the results for the LJ potential. In the figure there appear two branches, one at low and the other at high densities. The low density curve corresponds to the nonsolution line of the HNC which, as usual, precludes the determination of the spinodal. In this region the association degree is small, so little differences are expected between the corresponding low density

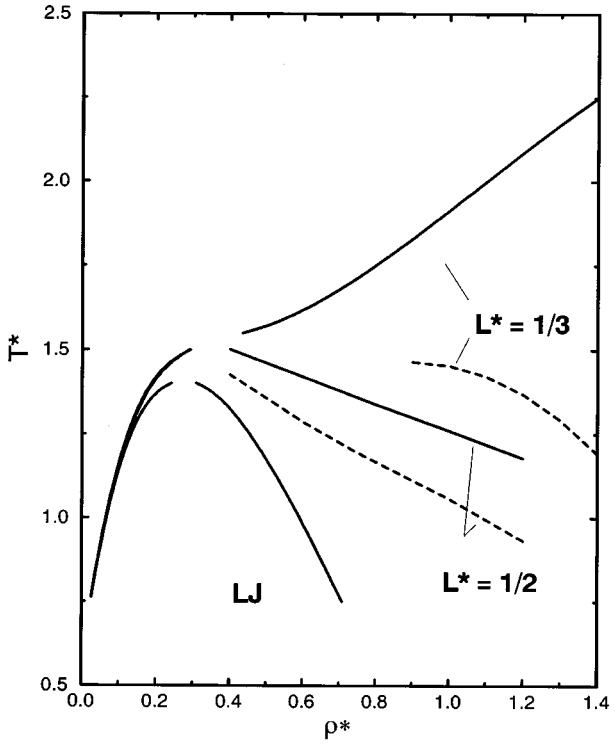

FIG. 3. Pseudospinodal lines for bond lengths $L^*=1/3$ and $L^*=1/2$ as predicted by the HNC integral equation. Solid lines refer to the CFM potential defined in Eq. (4) with $D_e^* = 0$ and dashed lines are for the same potential but fulfilling the steric saturation condition (see the text for details). The curves for the simple LJ potential are included for comparison.

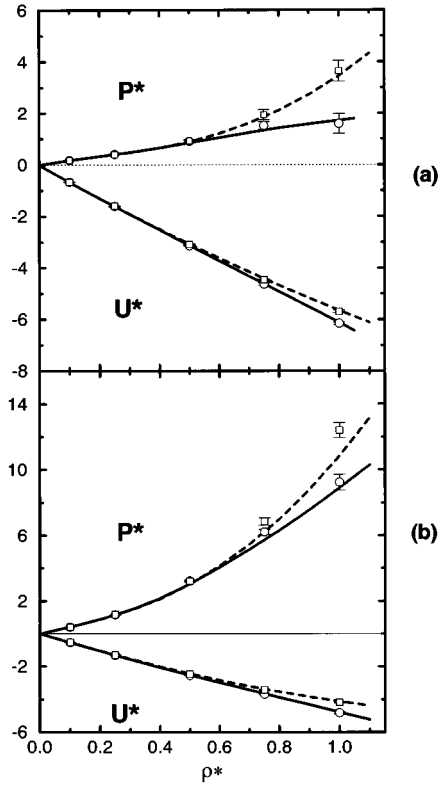

FIG. 4. Reduced internal energy and pressure for isotherms (a) $T^*=2$ and (b) $T^*=4$ of the system with $D_e^* = 0$. Lines correspond to HNC integral equation results for $L^*=1/3$ (solid) and $L^*=1/2$ (dashed). Symbols represent MC simulations for $L^*=1/3$ (circles) and $L^*=1/2$ (squares).

pseudospinodal lines of the LJ and that of the associating potential considered here. Notice in Fig. 3 that all of the nonsolution curves (irrespective of the bond length of the system) merge as the density becomes lower, with appreciable differences arising at larger densities where the association is favored. But, as stated above, we are more interested on the high density region for which the HNC pseudospinodal closely resembles a true spinodal line. We analyze this issue in what follows.

From Fig. 3 it is clear that the association works in the sense that the liquid phase is shifted to higher densities. Besides, our results suggest that the liquid may become completely unstable for short bond lengths, the phase diagram being then *probably* reduced to a fluid–solid equilibrium. It should be noted that this equilibrium may be altered by both the bond length and the well width (see Fig. 2). By comparing the reduced inverse isothermal compressibility χ_T^{-1} obtained from the widths used for Fig. 2(b), one could argue that the origin of the liquid instability is due to a wider potential width which favors association. This cannot be considered the main factor acting here since, at the same density and temperature, an elongation $L^*=1/2$ gives a higher level of association with the system remaining in a liquid phase. It is thus the competition between association and elongation which translates into the disappearance of the liquid region. In other words, the effect seems to be linked to the limited number of clusters that may appear at short bond lengths (recall that for $L^*=1/3$, the tetramer is the largest cluster that can be formed). In Fig. 3 we have also included the pseudospinodal curve obtained when the steric saturation case is enforced. In such a case the liquid phase would be stable. This fact also gives support to a possible relation between the topology of the species and the peculiar behavior observed for the shorter elongation analyzed in this work. For larger elongations the steric saturation works in the same direction, i.e., the liquid is stable in a larger range of temperatures and densities. What is apparent from these results is that association plays a central role in determining the phase behavior of simple systems and could help to explain some of the peculiarities observed for instance in dipolar and ionic systems.

B. Structure

In order to investigate the accuracy of the HNC integral equation in the description of the associating system, we have carried out several Monte Carlo (MC) simulations using the set of parameters mentioned above for the description of the intramolecular contribution to the potential energy ($k^*=15\,000$ and $D_e^* = 0$). We consider two isotherms, $T^*=2$ and $T^*=4$. Both correspond to supercritical systems, although the former temperature is in the vicinity of the pseudospinodal line for systems with elongation $L^*=1/3$ when the density is close $\rho^*=1.0$. Figure 4 depicts the internal energy and pressure obtained from HNC and MC calcula-

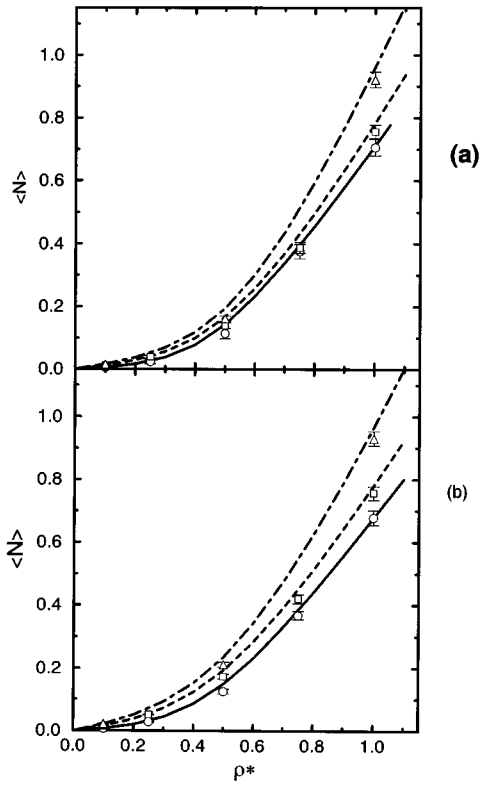

FIG. 5. Running coordination number, $\langle N \rangle$, for isotherms (a) $T^*=2$ and (b) $T^*=4$ and bond lengths $L^*=1/3$, $L^*=1/2$, and $L^*=3/5$ (system with $D_e^* = 0$). Lines and symbols have the same meaning than those in Fig. 4 with the addition of triangles and dash–dotted lines for $L^*=3/5$.

TABLE II. Running coordination numbers for the central force model with $D_e^* = 0$ from Monte Carlo and HNC integral equation.

		$T^*=2$		$T^*=4$	
L^*	ρ^*	MC	HNC	MC	HNC
	0.10	0.0056±0.0004	0.0057	0.0074±0.0005	0.0075
	0.25	0.024±0.007	0.026	0.028±0.002	0.031
1/3	0.50	0.115±0.017	0.144	0.125±0.008	0.149
	0.75	0.375±0.023	0.397	0.367±0.013	0.384
	1.00	0.706±0.027	0.711	0.678±0.024	0.677
	0.10	0.011±0.001	0.011	0.015±0.001	0.015
	0.25	0.039±0.004	0.041	0.051±0.002	0.053
1/2	0.50	0.140±0.009	0.168	0.174±0.008	0.193
	0.75	0.388±0.018	0.432	0.420±0.015	0.450
	1.00	0.756±0.021	0.783	0.757±0.021	0.780
	0.10	0.015±0.001	0.015	0.021±0.001	0.021
	0.25	⋯	0.052	⋯	0.070
3/5	0.50	0.162±0.009	0.195	0.212±0.008	0.236
	0.75	⋯	0.513	⋯	0.547
	1.00	0.921±0.025	0.961	0.930±0.023	0.966

tions. The results from theory and simulation are in excellent agreement, even at the highest densities considered. This coincidence is curious given the poor performance of the HNC for LJ potentials. In some sense this resembles the behavior of the HNC in ionic fluids. Notice that the simulation pressures for $T^*=2$ and $L^*=1/3$ show a change in the slope in agreement with the theoretical predictions. Therefore, the region of instability depicted in Fig. 3 is not a mere artifact of the HNC and one can be confident that the liquid phase becomes unstable at short elongations. Preliminary computations of the phase coexistence for such a Hamiltonian by means of the Gibbs ensemble Monte Carlo technique confirm this result.

Figure 5 represents the values of $\langle N \rangle$ obtained from the HNC and Monte Carlo simulations for the isotherms $T^*=2$ and $T^*=4$ and the bond lengths $L^*=1/3$, 1/2, and 3/5. Numerical results are collected in Table II. We have used $R_b=0.75\sigma$ as the upper integration limit in the computation of the running coordination number. At this distance the pair correlation function $g(r)$ is zero for all the elongations considered (see Fig. 6). For a given temperature, $\langle N \rangle$ increases with density, which is related with the increasing encounter probability of two particles as the system volume decreases. As could be expected, $\langle N \rangle$ increases with elongation for a given temperature. It is a manifestation of the simple fact that particles can establish links with more neighbors as the steric hindrance decreases. This behavior is present in both the simulation and the HNC results. The latter always overestimates the MC value for $\langle N \rangle$, as seen in Fig. 5 and Table II.

In Fig. 6 we present the pair correlation functions at $\rho^*=1.0$ and $T^*=2$ and the three elongations mentioned above. This large density is interesting because the system presents a high degree of association—$\langle N \rangle$ is larger than 0.7

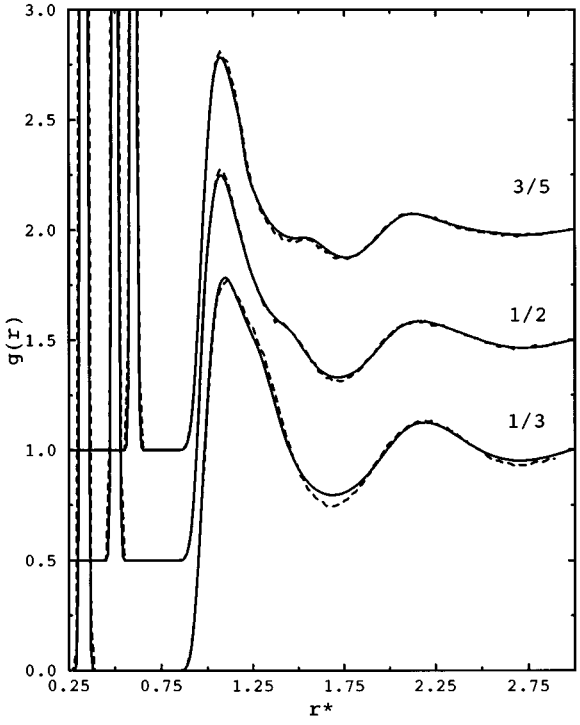

FIG. 6. Pair distribution functions for the system with $D_e^* = 0$ at $\rho^*=1.0$ and $T^*=2$ for bond lengths $L^*=1/3$, 1/2, and 3/5. The latter functions are shifted along the y axis. Solid lines represent HNC results and dashed lines MC simulations.

TABLE III. Monte Carlo cluster population expressed as the probability that a given particle belongs to a cluster of size n ($D_e^* = 0$ unless otherwise indicated).

		$T^*=2$				$T^*=4$			
L^*	ρ^*	$n=1$	$n=2$	$n=3$	$1-\Sigma_{n=1}^{3}$	$n=1$	$n=2$	$n=3$	$1-\Sigma_{n=1}^{3}$
1/3	0.10	0.994	0.006	⋯	⋯	0.993	0.007	0.000	⋯
	0.50	0.885	0.114	0.001	⋯	0.875	0.124	0.001	⋯
	1.00	0.349	0.596	0.055	⋯	0.373	0.575	0.052	0.000
	1.00[a]	⋯	⋯	⋯	⋯	0.245	0.504	0.228	0.023
1/2	0.10	0.990	0.010	0.000	⋯	0.984	0.016	⋯	⋯
	0.50	0.863	0.134	0.003	0.000	0.828	0.166	0.006	0.000
	1.00	0.317	0.546	0.115	0.022	0.336	0.482	0.144	0.038
	0.50[a]	⋯	⋯	⋯	⋯	0.329	0.347	0.238	0.086
	1.00[a]	0.218	0.505	0.240	0.037	0.232	0.446	0.238	0.084
3/5	0.10	0.986	0.014	0.000	⋯	0.977	0.022	0.000	⋯
	0.50	0.845	0.138	0.015	0.002	0.797	0.175	0.024	0.004
	1.00	0.290	0.303	0.178	0.229	0.294	0.293	0.173	0.240
	0.50[a]	⋯	⋯	⋯	⋯	0.337	0.249	0.160	0.254
	1.00[a]	0.274	0.284	0.185	0.257	0.276	0.278	0.176	0.270

[a]Full association limit.

in all cases—and, in some sense, it can give a hint on how well the molecular system will be described. The structure predicted by the theory is in very good agreement with the Monte Carlo simulations, in accordance with what we found for the thermodynamic quantities. The structure of the liquid is quite sensitive to the bond length in the same way as in real systems composed of homonuclear diatomic molecules of similar elongations. The molecular nature of the system is structurally denoted by the existence of secondary peaks (humps) at distances $r \approx L+\sigma$. Despite the great similarity between these pair correlation functions and those of true molecular models, it should be pointed out that the peaks observed around $L+\sigma$ are—for elongations 1/2 and 3/5—due in part to the formation of n-mers ($n>2$) which are not allowed in true molecular systems. This question will be addressed in more detail in what follows.

The averaged quantity $\langle N \rangle$ incorporates various contributions, from dimers to larger clusters. Simulation provides an easy route to obtain the cluster population. One only needs to define the *clustering distance*, $R_b=0.75\sigma$ in our case, and simply count the number of clusters of different sizes in a given configuration generated in the simulation. The analysis, extended over a large number of configurations, allows us to get the average value for the cluster population of the system. The method is the same we employed in a previous work dealing with ionic systems.[26] The cluster population, calculated from averages over 500 configurations, is reported in Table III. For $T^*=2$, the shorter bond length almost exclusively renders dimers as the largest cluster, even at the highest density. Increasing the elongation leads to the appearance of larger clusters. These also contribute very little to the overall population for $L^*=1/2$, but for $L^*=3/5$ their contribution is by no means negligible. Thus, for the shorter elongation ($L^*=1/3$), if the density and temperature are such that $\langle N \rangle$ is close to unity, one can approximately speak of a molecular fluid with small deviations due to the formation of high order clusters. At larger bond lengths ($L^*=1/2,3/5$) the situation would rather be similar to a polydisperse polymeric system. On the other hand, temperature has the effect of flattening the distribution curve, i.e., it decreases the population of the more abundant species and increases the number of other cluster types.

Once the clusters have been obtained for every MC configuration, it is easy to obtain the pair connectedness function, $p(r)$. This function has shown to be useful in describing association phenomena in liquid systems (see for instance its application to ionic association in electrolyte solutions[26]). In essence, $p(r)$ is similar to the pair correlation function $g(r)$ but it takes into account only particles within a cluster, i.e., particles that are directly or indirectly linked to the reference one. Therefore, $p(r)$ depends on the clustering distance, R_b. Since all the particles lying at a distance shorter than R_b are directly linked to the central one, it follows that the pair connectedness and the pair correlation functions are identical for $r<R_b$. In Fig. 7 we represent $p(r)$ for elongations $L^*=1/2$ and $L^*=3/5$ at $T^*=2$ and $\rho^*=1.0$. Let us discuss the $L^*=1/3$ case before commenting on the results of Fig. 7. Because of the potential and clustering definitions, for $L^*=1/3$ the maximum size of the higher order clusters is 4, with every particle separated from each other at a distance L^* in a tetrahedral arrangement. Therefore, $p(r)$ is identically zero outside the intramolecular region. This tells us that the shoulder observed in the pair correlation function (cf. Fig. 6) is of intermolecular origin.

The pair connectedness functions depicted in Fig. 7 present a sharp peak at a distance $r^* \approx 1$. The peak is due to the formation of trimers, which are essentially linear for $L^*=1/2$ and angular for $L^*=3/5$. In the latter case, given the longer separation between particles within the cluster, these may arrange themselves such that particles at the extremes lie at distances $r^* \approx 2^{1/6}$ (at the minimum of the intermolecular LJ potential contribution). For both elongations, the pair connectedness presents a second maximum at separations close to $L+\sigma$. This reflects an indirect link between two

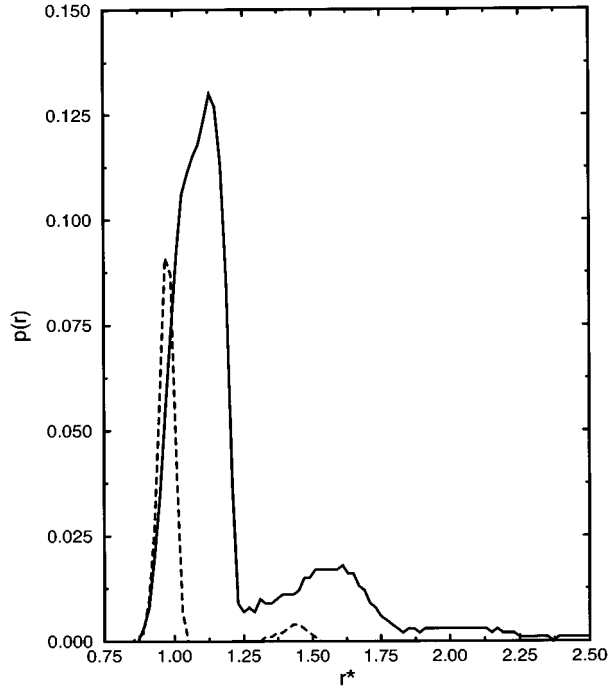

FIG. 7. Monte Carlo pair connectedness function for the systems and states of Fig. 6. Solid lines correspond to $L^*=3/5$ and dashed to $L^*=1/2$.

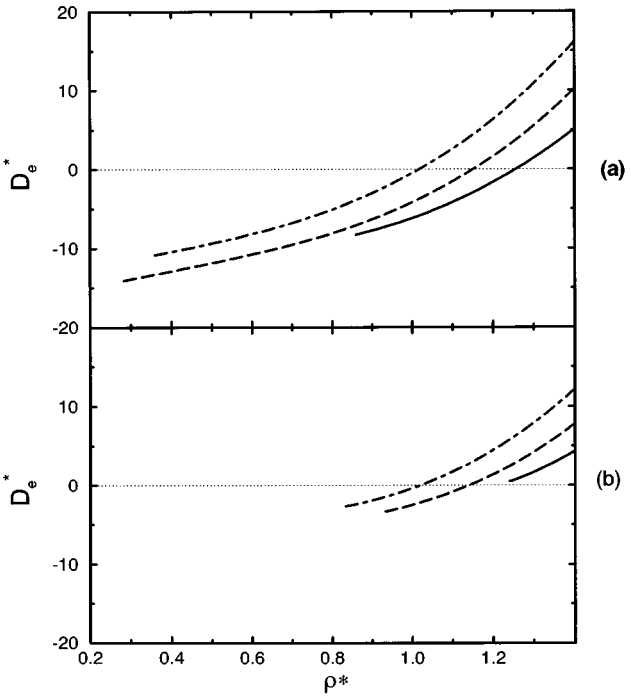

FIG. 8. Values of intramolecular potential depth, D_e^* leading to complete association ($\langle N\rangle=1$) within the HNC integral equation framework at temperatures (a) $T^*=4$ and (b) $T^*=2$. Solid lines, $L^*=1/3$; dashed, $L^*=1/2$; dash–dotted $L^*=3/5$.

particles mediated by a chain of at least two bonded particles (i.e., the cluster is made up of, at least, four particles). It is also to be noticed that in the case of the larger elongation $p(r)$ has a small but non-negligible value for separations longer than 2.5σ, which is a somewhat unexpected result in view of the small number of high order clusters (see Table III). Thus, $p(r)$ supports the idea that the topology of the clusters in systems with medium to large elongations is likely linear, with some deviations evidenced by the variations in width and position of the pair connectedness peaks. The peak around $L+\sigma$ is, in part, due to intracluster correlations but this contribution to $g(r)$ is smaller than that due to particles which belong to different molecules.

VI. THE COMPLETE ASSOCIATION LIMIT

A. Calculation of D_e and general properties

Now we will focus on a particular case of the association reaction, namely, the complete association limit. As mentioned above, it is possible to tune the equilibrium reaction by varying the intramolecular potential width and/or the location of the minimum of the intramolecular potential. Likewise, for a given width and elongation, the equilibrium can be altered by modifying the depth of the intramolecular potential well. As discussed in previous sections, $\langle N\rangle=1$ is a necessary but not sufficient condition to define a system exclusively made up of dimers. In order to establish such a limit, the Hamiltonian that defines the system should have the property of steric saturation. We have seen in the cluster analysis reported in the previous section that for short elongations, $L^*=1/3$ and $L^*=1/2$, the population of aggregates composed of more than two particles is quite small. It is for the larger elongation where there appear to be a significant number of large clusters (cf. Table III).

By solving the OZ integral equation coupled with the HNC closure, we have obtained the set of D_e^* values that fulfills the condition $\langle N\rangle=1$ as a function of density and temperature. In Fig. 8 these values are depicted for the temperatures $T^*=4$ and $T^*=2$. D_e^* takes both negative and positive values. The negative values point out that at the density and temperature under consideration the value of $\langle N\rangle$, before adjustment of D_e^*, is lower than one. Similarly the positive values correspond to systems that exhibit a value of $\langle N\rangle$ larger than one. All these lines end at the nonsolution curve of the HNC equation. In the case of steric saturation, D_e^* must have negative values. We have simulated the central force model potential using the set of D_e^* values furnished by the integral equation as seen above. From our previous results, one cannot expect to get a simulated value of $\langle N\rangle$ identical to one but we can be confident that its value will be quite close to the desired one. In Table IV we report the values obtained in the simulations for $\langle N\rangle$ as well as the D_e^* value for several selected thermodynamic conditions. Also reported are the simulated internal energy and pressure. The average running coordination numbers lie mostly below unity in accordance with the overestimation of $\langle N\rangle$ by the integral equation. Hence, a more negative value for D_e^* would be needed in order to fulfill the complete association condition. Nevertheless, it is to be expected that these small

TABLE IV. Thermodynamic properties and running coordination numbers in the full association limit ($\langle N\rangle=1$).

			U^*		P^*		$\langle N\rangle$		
L^*	ρ^*	T^*	MC	HNC	MC	HNC	MC	HNC	$-D_e^*$
1/3	1.0	4	-8.03 ± 0.15	-7.90	5.6 ± 0.6	4.9	1.03 ± 0.04	1.00	6.18
	0.5	4	-7.54 ± 0.24	-7.60	3.2 ± 0.3	1.3	0.99 ± 0.05	1.00	11.86
1/2	1.0	4	-6.15 ± 0.08	-6.17	11.0 ± 0.6	7.8	0.98 ± 0.03	1.00	4.19
	1.0	2	-6.83 ± 0.06	-6.86	2.4 ± 0.5	1.6	0.98 ± 0.03	1.00	2.51
	0.5	4	-6.30 ± 0.18	-6.40	3.4 ± 0.2	1.3	0.98 ± 0.04	1.00	9.35
3/5	1.0	4	-4.24 ± 0.07	-4.20	11.5 ± 0.6	10.1	0.98 ± 0.03	1.00	0.53
	1.0	2	-5.72 ± 0.05	-5.69	3.3 ± 0.6	3.1	0.97 ± 0.04	1.00	0.38

differences have a negligible influence on the properties of the system.

It is interesting to examine the ability of the integral equation to describe the thermodynamics of the system. In Fig. 9 we plot the thermodynamic properties for the states considered in Fig. 8 (numerical results are compiled in Table IV). The internal energy is predicted reasonably well by the HNC integral equation irrespective of the bond length. For pressure there are some discrepancies, although the HNC correctly predicts the trends observed in simulation. Notice in particular that the theory correctly describes the dependence on density for systems with different bond length. At the same density and temperature, the internal energy becomes more negative with increasing elongation. This may be a trivial consequence of the value of D_e^* used for the different systems. Pressure increases as the bond length is augmented. As can be expected, the association diminishes the system pressure and the same applies to a shortening of the bond length.

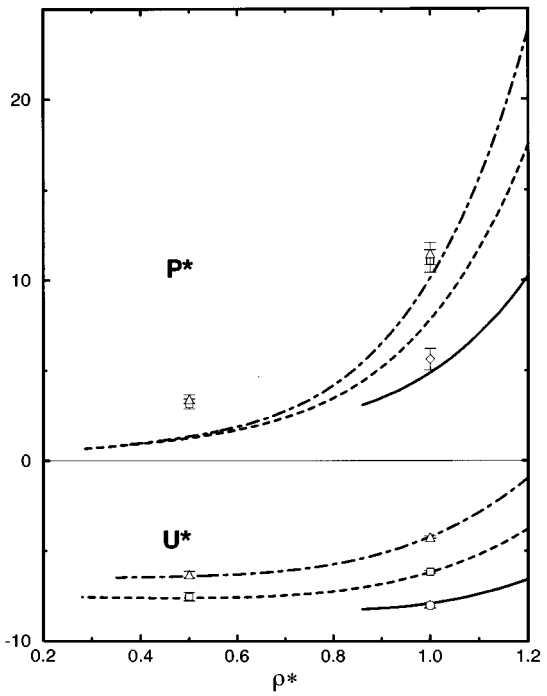

FIG. 9. Pressure and internal energy of systems in the complete association limit (i.e., using for D_e^* the values of the previous figure) along the isotherm $T^*=4$. Symbols are used for simulation results and lines for HNC calculations. $L^*=1/3$: solid, circles; $L^*=1/2$: dashed, squares; and $L^*=3/5$: dash–dotted, triangles.

We have performed the cluster analysis of the systems referred in Table IV in order to know which are the species that result from enforcing the constraint of full association, $\langle N\rangle=1$. The results are also compiled in Table III. As the running coordination numbers of the systems not fulfilling the condition are always less than unity (see Table II), the increase in the number of trimers and higher order clusters when the condition is imposed is a trivial result. Nevertheless, the simultaneous decrease in the number of dimers is significant. Thus, the complete association limit leads to a cluster population which does not resemble a system of diatomic molecules despite that, in both cases, $\langle N\rangle=1$. The effect of density is also to be noticed. Systems at constant T^* and L^* have approximately the same number of trimers and higher order clusters. On the contrary, the number of monomers and dimers can be rather different. A careful analysis indicates that the full association limit is reached in systems at low densities through the maximum saturation of the bonds within the complex clusters. At higher densities the increase in the probability of encounters between monomers leads to an increase in the population of dimers. In these conditions, the saturation of the bonds within higher order clusters is not needed. In other words, trimers and higher order clusters are preferably cyclic at low densities, whereas in dense systems these clusters are (topologically) more linear.

As to the pair correlation functions of the systems considered above, in Fig. 10 we compare the results obtained in the MC simulations with the HNC integral equation calculations for the bond lengths $L^*=1/3$, 1/2, and 3/5 at $T^*=4$ and $\rho^*=1.0$. The theoretical predictions show an excellent agreement with the simulation results. In addition we have included the correlation functions obtained in a molecular dynamics run. The simulation was initiated from a configuration of diatomics arranged in a fcc lattice. In these conditions molecules do not dissociate due to the large thermal barrier between intramolecular and intermolecular potentials. We recall that the structure of the system obtained from this simulation is essentially the same as that obtained from a rigid model. From the cluster analysis of configura-

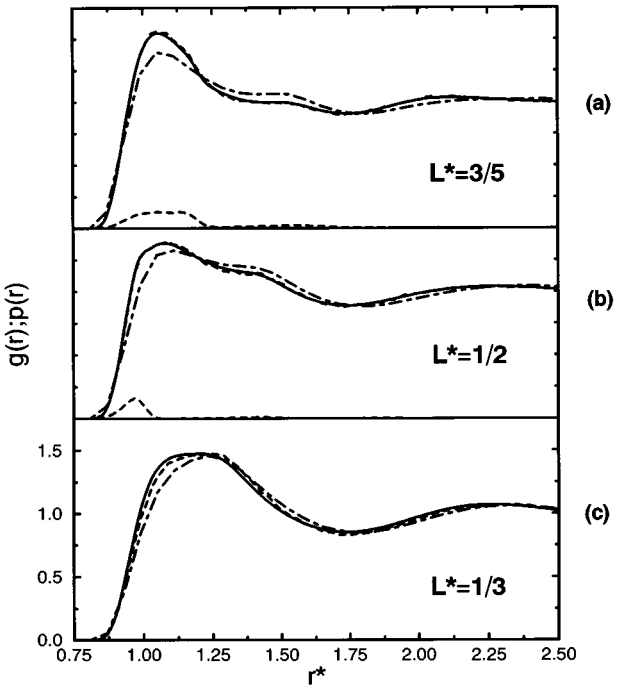

FIG. 10. Pair correlation functions for systems in the complete association limit at $T^*=4$ and $\rho^*=1.0$. Dashed lines, MC computations; solid, HNC predictions; dashed–dotted, molecular dynamics simulations for the same potential but with a starting configuration of particles clustered in dimers.

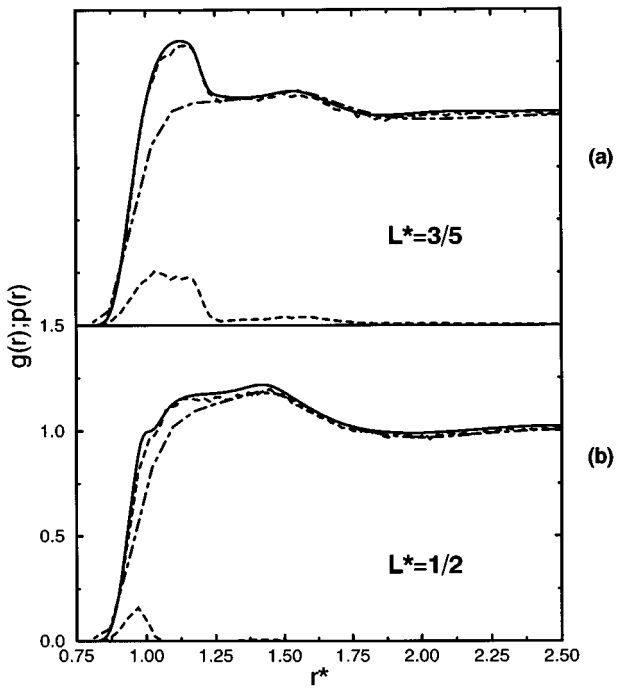

FIG. 11. As Fig. 10 but for $\rho^*=0.5$. The system with $L^*=1/3$ lies within the nonsolution region of the HNC theory and, thus, is not plotted.

tions obtained from the MC simulations we have concluded that, although dimers are dominant in the system, some perturbation with respect to the molecular fluid should be expected due to the presence of other species. The curves that result from the imposition of the $\langle N\rangle=1$ condition present some features typical of the molecular system as the shoulder around $L+\sigma$. This was also observed in $D_e=0$ case. The coincidence of the curves for the molecular system and the CFM for the shorter elongation $L^*=1/3$ is good, although the main peak is wider, indicating the presence of some more neighbors at shorter distances in the CFM than those observed in the molecular system. An increase in the bond length enhances the differences. Departures in position and magnitude of the peaks can be ascribed again to the contribution of higher order clusters denoted by the pair connectedness functions, also shown in Fig. 10.

Figure 11 presents the same functions as those in Fig. 10 but for a lower density $\rho^*=0.5$. The HNC nonsolution line precludes the computation of this thermodynamic state for $L^*=1/3$ so we report results just for elongations 1/2 and 3/5. The CFM results for $L^*=1/2$ are in good agreement with those for the molecular system, whereas for $L^*=3/5$ the CFM exhibits a large peak around $2^{1/6}\sigma$ absent in the molecular case. The pair connectedness reveals again that part of this contribution is due to the existence of clusters of size larger than two (trimers) which, as seen in Table III, are present in a significant quantity. Figure 11(a) shows that for $L^*=3/5$ the pair connectedness peaks at $2^{1/6}\sigma$ and $L+\sigma$ overlap. This stresses the variety of conformations exhibited by the large clusters formed in these conditions.

B. Comparison with molecular systems

Next we check the ability of the central force model to account for the properties of molecular models intended to describe real molecular fluids. We have focused on the structure of several homonuclear diatomic fluids that have been the subject of a recent work.[27] Again, the CFM are atomic systems, including an intermolecular contribution and an intramolecular component. The former is the same as the atom–atom potentials in the molecular diatomic models (see Table I) while the latter incorporates a value for D_e, enforcing the condition $\langle N\rangle=1$. The procedure for obtaining the D_e values for each system is the same as described above. The thermodynamic states lie in the neighborhood of the liquid branch of the gas–liquid equilibrium curves of N_2 and Cl_2. They are collected in Table V, together with the values for D_e. Notice that most of the states correspond to densities and temperatures respectively higher and lower than those considered in the previous sections.

Figures 12 and 13 show the atom–atom distribution functions of N_2 (at 66.4 and 77 K) and Cl_2 (at 200 and 290 K), respectively. We compare our results with computations for the diatomic model using the RISM-HNC integral equa-

TABLE V. Thermodynamic states of real systems considered in this work.

Molecule	T/K	T^*	ρ/(gr/cm^3)	ρ^*	D_e^*
N_2	66.4	1.780	0.8541	1.3319	2.30
N_2	77.0	2.064	0.8080	1.2600	0.72
Cl_2	200.0	1.153	1.6600	1.0631	0.64
Cl_2	290.0	1.671	1.4188	0.9086	−1.46

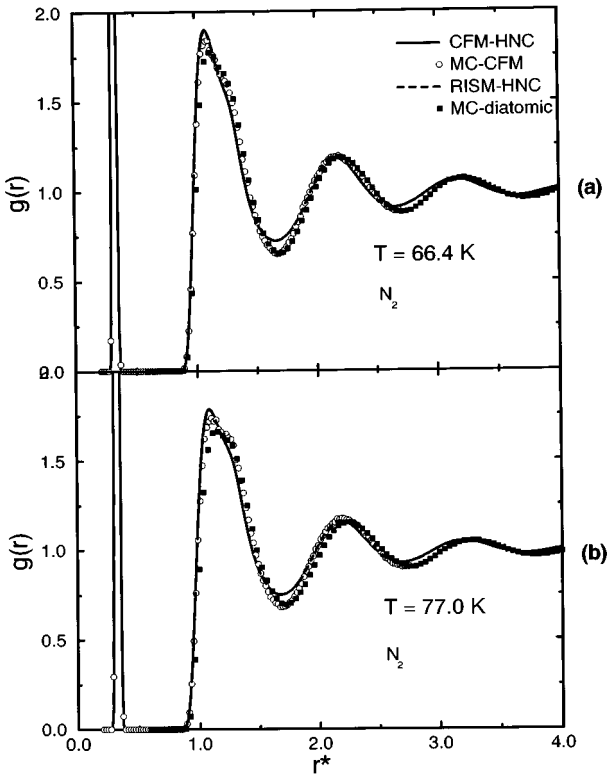

FIG. 12. Pair correlation functions for liquid N_2 in the vicinity of the liquid–vapor coexistence line. (a) $T=66.4$ K, $\rho=0.8541$ g/cm^3; and (b) $T=70$ K, $\rho=0.8080$ g/cm^3. Solid lines (HNC) and circles (MC simulation) represent results for the central force model proposed in this work (see Table I for the potential parameters). Filled squares and dashed lines represent MC and RISM-HNC calculations respectively for a true molecular (atom–atom) potential (taken from Ref. 27). The results of the RISM-HNC theory are also depicted though they are indistinguishable form the CFM-HNC theory.

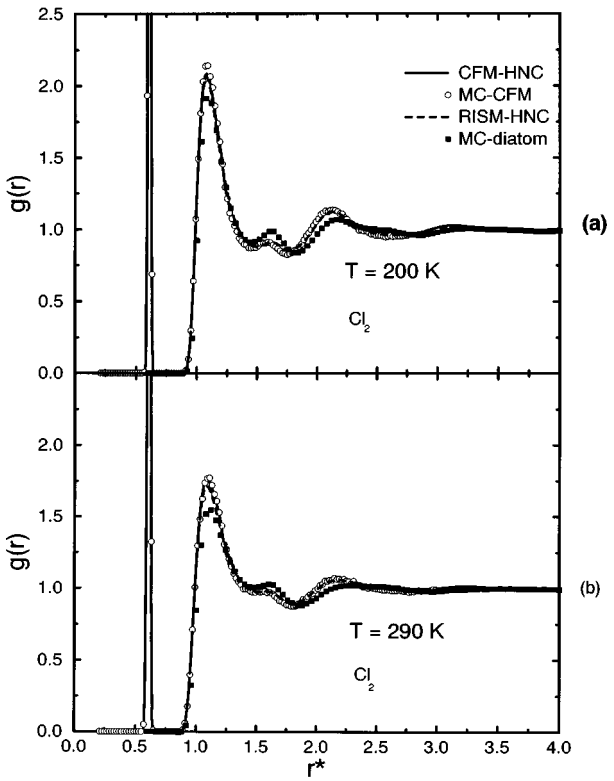

FIG. 13. Same as Fig. 12 but for Cl_2 at (a) $T^*=200$ K, $\rho=1.6600$ g/cm^3; and (b) $T^*=290$ K, $\rho=1.4188$ g/cm^3.

tion and MC simulation.[27] The structure obtained from the atomic HNC equation using the CFM potential is, for both liquids, almost indistinguishable from that predicted by the RISM-HNC for the molecular models. In some sense, it seems that the latter theory can be considered as a limiting case of a CFM when intramolecular potential is infinitely narrow, i.e., it is a Dirac's delta function. The comparison of theory with MC simulation results for the CFM potential at the same conditions of temperature, density, bond length, and D_e^* indicates that the HNC has some deficiencies in the prediction of the structure at low elongations (Fig. 12) but it is very reliable for larger bond lengths (Fig. 13).

The CFM-HNC results differ in several structural features from those of the molecular systems. Although the first peak is well predicted in both position and height, the magnitude of first minimum is not accurately described. Figures 12 and 13 demonstrate that the deficiencies are not due to the theoretical approximation but to the some inadequacy of the potential model in accounting for the molecular nature of the systems. This is clear when one observes the differences between the MC simulations of the CFM and the true diatomic fluid. In Table VI we report the cluster population for the states referenced in Table V. In N_2 at 66.4 K, dimers are clearly prevalent and the proportion of other species does not reach a 25%. Accordingly, there are little differences in this case between the molecular and the CFM systems [Fig. 12(a)]. The increase in temperature from 66.4 to 77 K translates in the formation of a small fraction of tetramers, also increasing the number of monomers and trimers at the cost of a subsequent reduction of dimers. As a result, the departures between the true molecular and the associated systems are slightly enhanced [Fig. 12(b)]. For more elongated diatomic molecules, the cluster population of the CFM differs very much from the strict dimerization. However, the deviations of the atom–atom distribution functions for the molecular system, with respect to the pair correlation functions of the associated one, do not correspond with their differences in the cluster population. In fact, Fig. 13 stresses the remarkable ability of the CFM system to ''emulate'' the molecular one.

TABLE VI. Monte Carlo cluster population for the real systems considered in this work.

Molecule	T/K	$n=1$	$n=2$	$n=3$	$1-\Sigma_{n=1}^{3}$
N_2	66.4	0.113	0.779	0.108	···
N_2	77.0	0.154	0.679	0.159	0.008
Cl_2	200.0	0.282	0.279	0.163	0.276
Cl_2	290.0	0.295	0.268	0.158	0.279

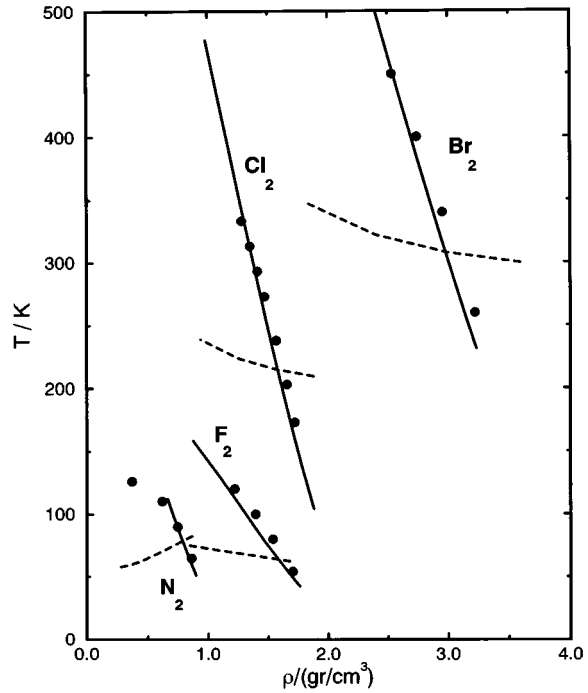

FIG. 14. Pseudospinodal lines of the HNC integral equation for the system in the complete association limit (solid lines) compared with the liquid branch of the liquid–vapor coexistence curves of several homonuclear diatomic molecules (full circles). Dashed lines are the HNC results for the corresponding associating systems with $D_e^* = 0$. The parameters given in Table I were used.

C. Stability boundaries in the complete association limit

In this section we discuss the pseudospinodal curves obtained from the HNC integral equation solved in the full association limit, i.e., after imposing the $\langle N \rangle = 1$ condition. The results are presented in Fig. 14. There we have also included the pseudospinodal lines obtained when the integral equation is solved without constraints for $\langle N \rangle$. The changes in the value of D_e^* have dramatic consequences on the stability region of the system. In general, the effect of a decrease in D_e^* is to shift the stability region of the liquid to larger densities and lower temperatures. The stability region of the liquid at intermediate densities and the gas phase are not accessible through the HNC approximation. This fact somehow resembles what happens with the HNC integral equation in the study of the restricted primitive model of electrolytes. In Fig. 14 we also plot the experimental liquid branch of the gas–liquid coexistence curve of diatomic molecular fluids. Even though the pseudospinodal lines lie inside the experimental liquid branch, as it should be if that would be the real spinodal line, one should not draw a definite conclusion in view of these curves. However, the coincidence in the slope of the curves is highly significant. It seems that our system composed of monomers, dimers, and larger clusters (polymeric species) actually presents a stability region which is closely related with that of a molecular system.

As has been commented along this work, the use of a potential which fulfills the steric saturation condition would warrant, for short enough elongations, $L^*=1/3$ for instance, that the only species present in the system would be dimers. A Hamiltonian that fulfills this requisite is easily built by considering the system as composed of two different types of atoms and by defining the intramolecular interactions a way such that association between like atoms is not possible. We have calculated the pseudospinodal curve resulting from the HNC integral equation for such a Hamiltonian. The pseudospinodal lines are virtually identical to those of the homogeneous reaction and for that reason are not shown here.

VII. SUMMARY AND DISCUSSION

In this work we have studied a *homogeneous* association reaction. The particles interact through a central force model potential, composed of an intermolecular component described by a Lennard-Jones interaction and an intramolecular potential defined by a harmonic oscillator. The atomic Ornstein–Zernike (OZ) integral equation coupled with the HNC closure turns out to be rather accurate for describing the thermodynamic properties, structure, and association as compared with Monte Carlo simulations of the same potential model. The study of the stability of the liquid and gas phases through the computation of the HNC pseudospinodal curve reveals that the stability region of this system is highly dependent on the bond length and the intramolecular potential depth. For a short elongation, such as $L^*=1/3$, the liquid phase is probably not stable and one can presume a direct gas–solid transition. These features can be related to the fact that, when particles associate, the available volume per particle increases. Aside from association effects, a short elongation imposes a limit on the topology and size of the clusters, and this also plays an important role on the stability of the system. In fact, we have observed that the liquid phase is recovered when a Hamiltonian ensuring the steric saturation condition is used. On the other hand, an increase in the bond length, at least up to the values considered in this work, also makes stable the liquid phase. It seems that further study of the stability boundaries of this model can throw some light on the conditions for the existence of the the vapor–liquid transition, a question that has recently received some attention, especially in the context of fluids made of associating particles as colloids or ionic liquids. Calculations for our model using the Gibbs ensemble will be reported in a forthcoming publication.

The central force potential considered here is also used to model molecular systems. We have assessed its ability to describe the structure and thermodynamics of homonuclear diatomic molecular fluids, such as N_2 and the halogens. In a true diatomic molecular system the number of bonds per particle is exactly one. One can enforce this condition on the integral equation but only on average because the CFM does not guarantee steric saturation. Despite this limitation we have studied the effect of imposing the condition $\langle N \rangle = 1$ (referred to as the complete association limit) on the theory. In order to solve the integral equation we have devised a simple Newton–Raphson procedure which adjusts the num-

ber of bonds per particle (the intramolecular coordination number) to the desired value. The adjustment of the average number of bonds per particle is feasible by making the intramolecular potential more or less attractive. Comparison with Monte Carlo simulation shows that the HNC theory works very well in predicting the structure of the system as well as the internal energy. As usual, the pressure is the quantity which presents the larger discrepancies. We have also solved the HNC integral equation in combination with the full association condition, $\langle N\rangle=1$, for thermodynamic states typical of the liquid state. Comparison with molecular theories shows than an atomic theory like this predicts a structure which is virtually the same as that obtained from a molecular theory such as the RISM-HNC.

Once the theory is checked satisfactorily against simulation, the next issue addressed in this work is to which extent the associating potential model is able to account for the properties of real molecular liquids, despite that systems fulfilling the complete association condition are noticeably polydisperse. The pair distribution functions of CFM models for N_2 and Cl_2 are quite similar those reported previously for atom–atom models. The features denoting a molecular structure are correctly predicted. However, there are small departures in the height of secondary peaks and the phase of the curves at large distances. Flory–Huggins, and also several recent studies,[28–31] has shown the insensitivity of the equation of state to polydispersity as long as the average chain length is the same. This argument can help to understand the coincidence between the HNC pseudospinodal curve of the CFM potential and the liquid branch of the experimental vapor–liquid coexistence line of N_2 and halogens.

One of the aims of this paper has been to analyze a possible route to solve molecular systems at the level of atomic theories by using central force model potentials. It's possible application to water is tempting being this the paradigm of associating fluid. From Monte Carlo simulations of the Stillinger's CFM of water, we know that it furnishes the correct number of intramolecular bonds at room temperature. This feature is not predicted by the atomic Ornstein–Zernike integral equation coupled with the HNC closure. The failure is due to the neglect of the bridge functions which play a main role in determining the correct number of bonds in the molecule. Recently, Vossen and Forstman[5] adjusted the intramolecular bonds by using empirical bridge functions in addition to the hard sphere ones. Thus, a possible theoretical route to the structure of water consists in the usual atomic HNC theory supplemented with the addition of an effective potential that ensures the fulfillment of the average number of intramolecular bonds. Under these circumstances one can expect to get reasonable results for the structure as it happens in a RISM-like treatment.[32] In our opinion, future work should be centered on the search of methods that render such effective potentials in a systematic (i.e., nonempirical) manner. An approach as that presented in this work may provide a sensible alternative along that way.

ACKNOWLEDGMENTS

This work was partially supported by Grants No. PB93-0085 and PB94-0112 furnished by the Dirección General de Investigación Científica y Tecnológica (DGICYT) of Spain. FB acknowledges a predoctoral fellowship awarded by the Universidad Complutense de Madrid.

[1] H. L. Lemberg and F. H. Stillinger, J. Chem. Phys. **62**, 1677 (1975); A. Rahman, F. H. Stillinger, and H. L. Lemberg, J. Chem. Phys. **63**, 5223 (1975); F. H. Stillinger and A. Rahman, J. Chem. Phys. **68**, 666 (1978).
[2] H. L. Lemberg and F. H. Stillinger, Mol. Phys. **32**, 353 (1976).
[3] R. A. Thuraisingham and H. L. Friedman J. Chem. Phys. **78**, 5772 (1983).
[4] T. Ichiye and D. J. Haymet J. Chem. Phys. **89**, 4315 (1988).
[5] M. Vossen and F. Forstman, J. Chem. Phys. **101**, 2379 (1994).
[6] M. S. Wertheim, J. Stat. Phys. **35**, 19 (1984); 35 (1984).
[7] M. S. Wertheim, J. Stat. Phys. **42**, 459 (1986); 477 (1986).
[8] W. R. Smith and I. Nezbeda, J. Chem. Phys. **81**, 3694 (1984); I. Nezbeda and G. A. Iglesias-Silva, Mol. Phys. **69**, 767 (1990); I. Nezbeda and W. R. Smith, J. Chem. Phys. **100**, 2191 (1994).
[9] W. G. Chapman, K. E. Gubbins, C. G. Joslin, and C. G. Gray, Fluid Phase Equil. **29**, 337 (1986); C. G. Joslin, C. G. Gray, W. G. Chapman, and K. E. Gubbins, Mol. Phys. **62**, 843 (1987); G. Jackson, W. G. Chapman, and K. E. Gubbins, *ibid.* **65**, 1 (1988); W. G. Chapman, G. Jackson, and K. E. Gubbins, *ibid.* **65**, 1057 (1988).
[10] P. T. Cummings and G. Stell, Mol. Phys. **51**, 253 (1984).
[11] P. T. Cummings and G. Stell, Mol. Phys. **55**, 33 (1985).
[12] Y. V. Kalyuzhnyi, G. Stell, M. L. Llano-Restrepo, W. G. Chapman, and M. F. Holovko, J. Chem. Phys. **101**, 7939 (1994).
[13] R. P. Sear and G. Jackson, J. Chem. Phys. **102**, 939 (1995).
[14] S. H. Lee, J. C. Rasaiah, and P. T. Cummings, J. Chem. Phys. **83**, 317 (1985); J. C. Rasaiah and S. H. Lee, *ibid.* **83**, 5870 (1985).
[15] S. H. Lee and J. C. Rasaiah, J. Chem. Phys. **86**, 983 (1987).
[16] Y. Zhou and G. Stell, J. Chem. Phys. **98**, 5777 (1993).
[17] D. Chandler and H. C. Andersen, J. Chem. Phys. **57**, 1930 (1972).
[18] L. J. Lowden and D. Chandler, J. Chem. Phys. **59**, 6586 (1973); **61**, 5228 (1974); P. T. Cummings, G. P. Morris, and C. C. Wright, *ibid.*, **86**, 1696 (1982).
[19] P. A. Monson, Mol. Phys. **47**, 435 (1982).
[20] P. S. Y. Cheung and J. G. Powles, Mol. Phys. **30**, 921 (1975).
[21] K. Singer, A. Taylor, and J. V. L. Singer, Mol. Phys. **33**, 1757 (1977); **37**, 1239 (1979); S. Romano and K. Singer, *ibid.* **37**, 1765 (1979); E. Detyna, J. V. L. Singer, K. Singer, and A. Taylor, *ibid.* **41**, 31 (1980).
[22] M. P. Allen and D. J. Tildesley, *Computer Simulation of Liquids* (Clarendon, Oxford, UK, 1987).
[23] J. M. Hayle, *Molecular Dynamics Simulation: Elementary Methods* (Wiley Interscience, New York, 1992).
[24] S. Labik, A. Malijevsky, and P. Vonka, Mol. Phys. **56**, 709 (1985).
[25] L. Belloni, J. Chem. Phys. **98**, 8080 (1993).
[26] F. Bresme and J. L. F. Abascal, J. Chem. Phys. **99**, 9037 (1993).
[27] C. Martín, M. Lombardero, M. Alvarez, and E. Lomba, J. Chem. Phys. **102**, 2092 (1995).
[28] M. S. Wertheim, J. Chem. Phys. **87**, 7323 (1987).
[29] W. G. Chapman, G. Jackson, and K. E. Gubbins, Mol. Phys. **65**, 1057 (1988).
[30] A. Hertanto and R. Dickman, J. Chem. Phys. **93**, 774 (1990).
[31] S. Phan, E. Kierlik, M. L. Rosinberg, H. Yu, and G. Stell, J. Chem. Phys. **99**, 5326 (1993).
[32] B. M. Pettitt and P. J. Rossky, J. Chem. Phys. **77**, 1451 (1982).